ARTICLE

C-term Magnetic Circular Dichroism (MCD) Spectroscopy in Paramagnetic Transition Metal and f-Element Organometallic Chemistry

Received 00th January 20xx,
Accepted 00th January 20xx

DOI: 10.1039/x0xx00000x

Nikki J. Wolford[a], Aleksa Radovic[a] and Michael L. Neidig[a]*

Magnetic circular dichroism (MCD) spectroscopy is a powerful experiment used to probe the electronic structure and bonding in paramagnetic metal-based complexes. While *C*-term MCD spectroscopy has been utilized in many areas of chemistry, it has been underutilized in studying paramagnetic organometallic transition metal and f-element complexes. From the analysis of isolated organometallic complexes to the study of in situ generated species, MCD can provide information regarding ligand interactions, oxidation and spin state, and geometry and coordination environment of paramagnetic species. The pratical aspects of this techique, such as air-free sample preparation and cryogenic experimental temperatures, allow for the study of highly unstable species, something that is often difficult with other spectroscopic techniques. This perspective highlights MCD studies of both transition metal and f-element organometallic complexes, including in situ generated reactive intermediates, to demonstrate the utility of this technique in probing electronic structure, bonding and mechanism in paramagnetic organometallic chemistry.

Introduction

Electronic structure and bonding in metal complexes is central to their fundamental properties and reactivities across materials, inorganic, organometallic and bioinorganic chemistry. Within organometallic chemistry, there has also been an increased focus on base metal organometallic complexes where paramagnetic ground states are more prevalent than in their precious metal analogues. Similar challenges exist in f-element organometallics, which have been of long-term interest in order to define the role of f-orbitals in bonding and reactivity. As such, techniques that can be utilized for evaluating electronic structure in such paramagnetic organometallics are particularly important as more traditional methods such as NMR are often less informative for such species. Magnetic circular dichroism (MCD) spectroscopy is a powerful method for evaluating electronic structure and bonding in paramagnetic organometallic complexes including insight into both excited and ground state splittings, oxidation and spin state, and geometry in a single spectroscopic method, including complexes with both Kramers (half-integer spin) and non-Kramers (integer spin) ground states. When combined with other spectroscopic probes, such as electron paramagnetic resonance (EPR) spectroscopy, Mössbauer spectroscopy, or theoretical insight, further electronic structure insight can be obtained as highlighted herein.

MCD spectroscopy combines the traditional circular dichroism (CD) experiment with a longitudinal magnetic field, as illustrated in Fig. 1. The addition of the magnetic field induces optical activity (chirality) via the Faraday effect, such that all species are MCD active.[1] There are several advantages to the use of MCD spectroscopy over traditional absorption spectroscopy, especially when probing metal-based transitions in paramagnetic organometallic complexes. First, since Δε, or the difference in absorption of left- and right- circularly polarized light, is signed, both CD and MCD spectroscopies can exhibit both positive and negative transitions. This often allows for the resolution and assignment of transitions which are often broad in absorption spectroscopy, as they may be resolved by sign in CD or MCD. Second, MCD spectra of materials with degenerate or nearly degenerate ground states have significant signal intensity at low temperature. This intensity is greater in complexes which have large spin orbit coupling (SOC) constants, such as those with paramagnetic metal centers, making MCD an ideal experiment for studying paramagnetic organometallic complexes. In addition, the magnetic field and temperature dependence of MCD transitions can be used to provide insight into the energy splitting of the ground state sublevels which, when related to ligand field theory, can provide structural information such as spin state, coordination number, and geometry.[2-7]

While MCD spectroscopy has historically been most widely utilized in bioinorganic systems containing paramagnetic metals[8-18], this experimental method is equally powerful for the elucidation of electronic structure information in paramagnetic organometallic systems. This is especially important for complexes which contain first row transition metals or f-elements due to the propensity of such organometallic systems to have unpaired electrons. The experiment also allows for in situ characterization of species which can be utilized to track species at various time points over the course of a reaction by freeze trapping the reaction at a specific time point. This allows for structural insight into species which cannot be isolated from reaction mixtures. This type of reaction tracking of paramagnetic intermediates has become more relevant as first-row transition metal catalysed transformations become more prominent. The cryogenic nature of the *C*-term MCD experiment also allows for the study of thermally sensitive species, an area where many other

[a] *Department of Chemistry, University of Rochester, Rochester, New York 14627, USA. *Email: neidig@chem.rochester.edu*

† Footnotes relating to the title and/or authors should appear here.

Electronic Supplementary Information (ESI) available: [details of any supplementary information available should be included here]. See DOI: 10.1039/x0xx00000x

spectroscopic techniques are not equipped to handle. Herein we present an overview of the theory behind the *C*-term MCD experiment as well as several examples of how *C*-term MCD has been utilized to provide electronic structure insight into paramagnetic transition metal and f-element organometallic chemistry.

The MCD Experiment

MCD spectroscopy combines the CD experiment with a magnetic field which runs parallel to the propagation direction of the circularly polarized light, as outlined in Fig. 1. The MCD setup at the University of Rochester is based around a commonly used design. This combines a split pair horizontal field superconducting magnet with a variable temperature sample insert which allows for variable temperature experiments from 1.6 K to 300 K at the sample. As with CD, MCD spectroscopy measures the difference between left- and right-circularly polarized (lcp and rcp) light quantified by the

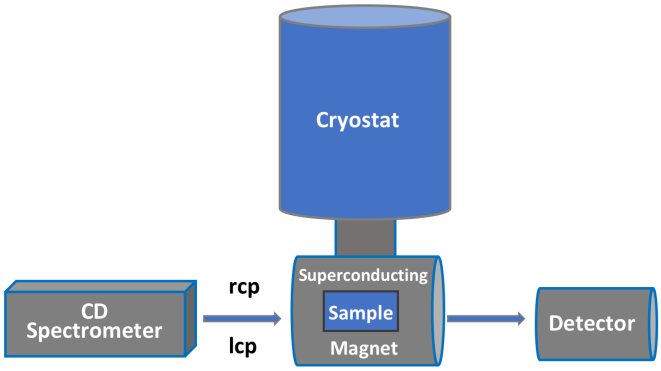

Fig 1. Schematic of a magnetic circular dichroism spectrometer.

extinction coefficients, ε_L and ε_R. This difference, Δε, relates to the difference between lcp and rcp absorbance, or ΔA, via Beer's Law. In CD, the selection rules require that the optical transition from the ground state to the excited state must be both electric dipole and magnetic dipole allowed along the same molecular direction. This selection rule can only be satisfied by complexes which belong to chiral point groups such as C_n, D_n, O, T, and I, or those with optical activity. Introduction of the longitudinal magnetic field in MCD spectroscopy induces optical activity in any material due to the Faraday effect, such that all substances exhibit MCD activity regardless of the structural arrangement of the atoms.

The intensity of an MCD spectrum is proportional to three contributions which are designated as *A*-, *B*-, and *C*-terms as shown in Equation 1. Here, ΔA is the field dependent difference between the absorption of left- and right-circularly polarized light, E is the energy of a photon (E = hν), α is the electric permeability, C is the concentration of the sample, ℓ is the path length of the sample cell, n is the index of refraction, β is the Bohr magneton, H is the applied magnetic field, *f*(*E*) is the absorption bandshape, and δ*f*(*E*) /δ*E* is its first derivative.

$$\frac{\Delta A}{E} = \frac{2N_0\pi^3\alpha^2 C\ell log e}{250hcn}\beta H\left[A_1\left(-\frac{\delta f(E)}{\delta E}\right) + \left(B_0 + \frac{C_0}{kT}\right)f(E)\right] \quad (1)$$

While all three of these mechanisms may contribute to the MCD spectrum for a paramagnetic species, the *C*-term is the largest contribution at room temperature and is approximately two orders of magnitude larger than other term contributions at cryogenic temperatures, dominating low-temperature measurements of

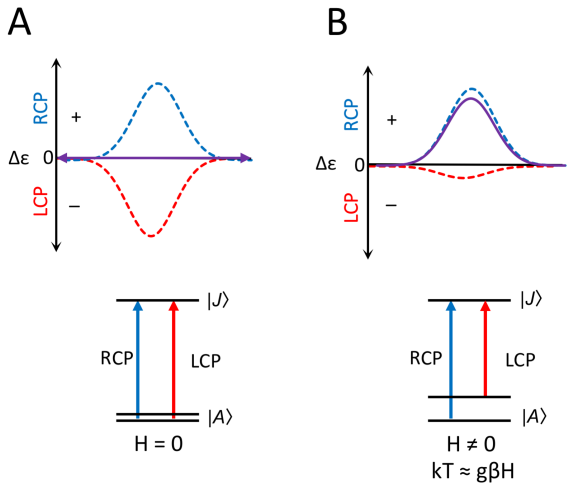

Fig 2. The *C*-term MCD intensity for a degenerate ground state system (A) in the absence and (B) in the presence of an applied magnetic field. Note that non-zero intensity occurs only in the presence of the magnetic field induced Zeeman splitting of the ground state.

paramagnets including paramagnetic organometallic complexes. The *C*-term mechanism requires a degenerate ground state and that the thermal energy (kT) be on the same order of magnitude as the Zeeman splitting (gβH) which is why cryogenic temperatures are utilized for this experiment. In the absence of the applied magnetic field, the ground state remains degenerate and the difference in absorption of the lcp and rcp transitions are the same, resulting in a cancellation of the signal as shown in Fig 2A. In the presence of the applied magnetic field, the ground state degeneracy is removed due to the Zeeman effect, which results in differing intensities in the lcp and rcp transitions such that they no longer cancel out, leading to an absorption band shape as shown in Fig 2B. Therefore, the *C*-term mechanism is both magnetic field and temperature dependent. This is due to the field dependence on the magnitude of the ground state splitting as well as the temperature dependence of the population of over the Zeeman split ground state.

A large contribution to *C*-term intensity originates from the presence of spin orbit coupling (SOC). This SOC effect is due to the requirement of two perpendicular transition dipole moments which are non-zero at the same time, as shown in Equation 2.

$$C_0 \propto g_z M_x M_y + g_y M_x M_z + g_x M_y M_z \quad (2)$$

In low symmetry sites, transitions between orbitally non-degenerate ground and excited states can only have a transition moment in a single direction which does not allow this requirement to be satisfied. The presence of SOC between two excited states with perpendicular transition dipole moments allows for some mixing of the two states, satisfying the requirement for the two perpendicular transition dipole moments and resulting in *C*-term intensity. As a result, transitions with significant metal character (i.e. d-d, f-f, LMCT, MLCT) will exhibit significant intensity in *C*-term MCD due to the large SOC constants of the metal. Concurrently, light atoms with smaller SOC constants, such as those common in organometallic ligand frameworks, will have less SOC. This means that transitions which have little or no metal character will be less intense in MCD. This aspect of MCD is advantageous when wanting to focus on the metal

center, as ligand-based transitions often dominate in traditional electronic absorption spectroscopy.

The *C*-term MCD experiment is often run across several energy regions, namely the near-infrared (NIR) and ultraviolet-visible (UV-Vis) regions. The low energy NIR region is where f-f and d-d transitions would be expected to be observed while the UV-Vis region contains metal to ligand and ligand to metal charge transfer (MLCT and LMCT) transitions. The information obtained from these spectra provide insight into the electronic structure, such as geometry, of the metal center as well as into metal-ligand bonding interactions. When combined with saturation magnetization experiments, the transitions in the NIR region can provide insight into oxidation state, spin state, and geometry about the metal center.

Beyond the insight into electronic excited states, evaluation of the temperature and magnetic field dependence of *C*-term MCD signals can provide ground state information for paramagnetic species. This subset of MCD is called saturation magnetization, or variable temperature variable field (VTVH) MCD. This experiment requires the collection of MCD intensities over a range of temperatures and magnetic fields at a fixed wavelength where an MCD transition was observed. Analysis of the VTVH MCD data can provide ground state spin Hamiltonian parameters for a given complex, insight which is often difficult to obtain for non-Kramers ground states. These ground state spin Hamiltonian parameters can then be used to determine the spin state as well as zero field splitting (ZFS) parameters of the complex corresponding to that specific transition. Since this experiment is performed at a single wavelength within the spectrum, it can also be used to determine the spin state and ZFS parameters of an individual species in a sample which may contain two or more paramagnetic complexes. In addition to spin state and ZFS parameters, in systems with Kramers ground states, VTVH MCD can also provide the polarizations of the transitions if the experimental g-values are known. Once the polarizations are obtained, the individual transitions can be assigned to specific metal-ligand interactions within the complex being investigated.

The practical aspects of the MCD experiment are also very beneficial to studies of paramagnetic organometallic complexes. Solid mull samples (i.e. finely ground powder samples which are mixed with a mulling agent) can be used for MCD, enabling studies on isolated or pure crystalline material of well-defined organometallic complexes. MCD samples can also be run as frozen solution glasses, which allows for in situ determination of species which may not be isolable, as well as tracking species at specific timepoints in reaction mixtures. This has proven very useful for tracking species in catalytic reactions as well as for assignment of spin state and geometry of transient reaction intermediates. MCD samples can readily be prepared in inert atmosphere gloveboxes, where handling of materials which are air, moisture and temperature sensitive have been successful. The experiment itself is performed at liquid helium temperatures and samples remain frozen at all times, which allows for characterization of species which are unstable, an area where many characterization techniques which provide similar information content, such as SQUID, are less available. This ability to both handle sample preparation as well as perform the experiment at low temperature and under inert atmosphere is ideal in organometallic chemistry, where complexes have been reported to be both temperature and air sensitive.

Despite the many benefits to utilizing MCD spectroscopy for studying paramagnetic organometallic complexes, the experiment remains underutilized for evaluating electronic structure and bonding paramagnetic organometallic compounds. The examples which do exist have provided important insight into both the mechanism of organometallic transition metal catalysed transformations as well as in the fundamental understanding of electronic structure and bonding in both transition metal and f-block chemistry. The ability to directly probe the spin state, oxidation state, and coordination geometry of the metal center provides valuable information about reactive intermediates of in situ generated samples. Combining the *C*-term MCD experiment with information obtained using other spectroscopic techniques, as well as theoretical calculations, can result in a detailed understanding of the bonding in paramagnetic organometallic species. This perspective outlines the application of *C*-term MCD to both d-block and f-element organometallics, providing examples of its use for identifying transient intermediates in d-block catalysis and the usability of the experiment for correlation of structure-reactivity. In addition, the more traditional use of *C*-term MCD for studies of the electronic structure and bonding in well-defined complexes of both d-block and f-element organometallic complexes are outlined.

Paramagnetic Transition Metal Organometallics

Insight into Reactivity and Mechanism in Paramagnetic Organometallic Transition Metal Catalysis

As the interest in performing catalytic transformations using early transition metals continues to grow, so does the need for spectroscopic techniques for understanding the underlying mechanism and speciation of these reactions. Early transition metal catalysts offer a more cost effective and, in some cases, less toxic alternative to precious metal catalysts for organic transformations such as C-C cross coupling while also demonstrating unique reactivity and selectivity that cannot be attained using precious metals. A fundamental understanding of the underlying mechanism in transition metal catalysed transformations is essential to achieving the same level of informed reaction development met by precious metal catalysis. One of the difficulties in studying these reactions is the tendency of the early transition metals to form highly paramagnetic intermediates. In recent years, *C*-term MCD spectroscopy has been utilized as a spectroscopic probe for these type of systems, as it can be used to study paramagnetic species which have been isolated, in situ reactions at specific timepoints, and the information set available from MCD can provide a better understanding of the electronic structure and bonding environment around active species in situ which may not be isolable. This has been demonstrated for a variety of transition metal catalysed C-C cross coupling reactions outlined herein, where MCD provided an understanding of reactive species, as well as trends in reactivity which allowed for improvement in the reaction mechanism.

In 2020, Park and co-workers utilized *C*-term MCD to investigate the correlation between the C-C cross-coupling activity of high valent nickel cycloneophyl complexes with the energies of the charge transfer (CT) transitions.[19] These high valent organometallic complexes have been found to be good targets for this type of study, as they show significant variation in the rate of reductive elimination for the formation of the same product depending instead on the oxidation state and supporting ligands of the transition metal center. The work of Park and co-workers combined MCD, electron paramagnetic resonance (EPR), X-ray absorption spectroscopy (XAS) and resonance Raman to investigate these CT energies with C-C bond formation. The NIR MCD spectra, in combination with EPR, was used to spectroscopically determine the structures, specifically the coordination numbers, of the high-valent Ni complexes after being cryoreduced. The UV-vis MCD spectra, in combination with the

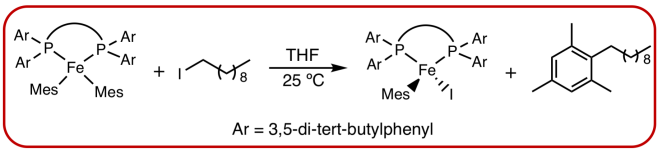

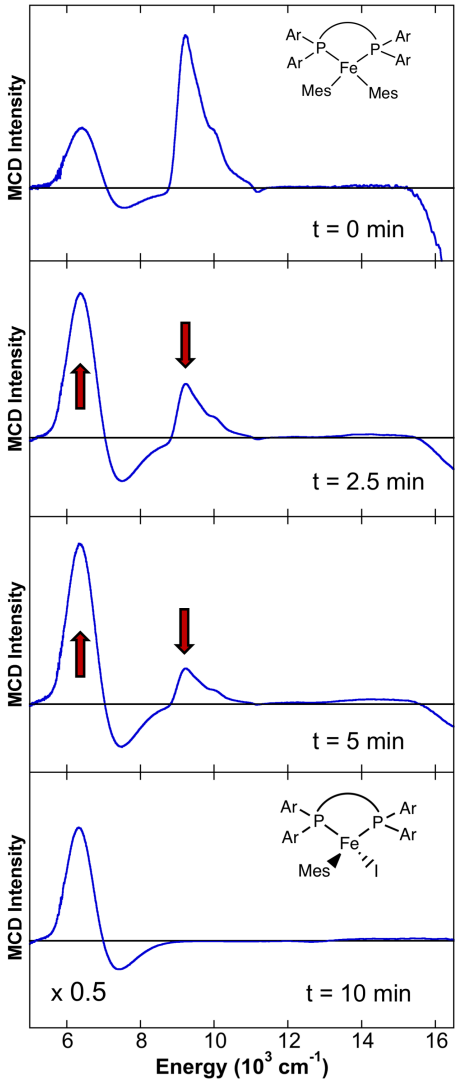

Fig 3. The 5 K, 7 T, NIR MCD spectrum of insitu generated $FeMes_2$(SciOPP) (top) and subsequent timepoints after the addition of 1-iododecane at 25 °C in THF, with arrows showing the consumption of $FeMes_2$(SciOPP) and formation of FeIMes(SciOPP). Adapted with permission from *J. Am. Chem. Soc.*, 2014, **136**, 9132-9143. Copyright 2014 American Chemical Society.

absorption spectra and TDDFT calculations, allowed for assignment of the observed charge transfer transitions. Overall, it was determined that the empirical correlations between the rate of C-C bond forming reductive elimination reactions and C-to-Ni CT transition energies of this series of cycloneophyl complexes originates from the fact that the reductive elimination and the C-to-Ni CT transitions involve the same frontier molecular orbitals. This correlation was then utilized when the C-to-Ni CT transitions were triggered using light of the appropriate energy to overcome the kinetic barrier of reductive elimination. This type of correlation between observed reactivity and spectroscopic data, and resultant improvement in reactivity, emphasizes the importance of understanding reaction mechanism at an electronic structure level.

C-term MCD spectroscopy has also been utilized to study the mechanism of iron-catalysed C-C cross-coupling reaction which utilize bisphosphine supporting ligands. In 2014, Neidig and co-workers reported the use of freeze-quenched spectroscopy to obtain information about iron speciation at specific time points in the Fe-SciOPP catalysed Kumada cross-coupling of MesMgBr and primary alkyl halides (Fig. 3).[20] The combined use of ^{57}Fe Mössbauer, *C*-term MCD spectroscopy, low temperature isolation and crystallization of key iron intermediates, and GC quantification of product formation, allowed for a deeper understanding of the on-cycle reactive species. It was determined that the addition of 1 equivalent of MesMgBr to $FeCl_2$(SciOPP) resulted in a 5 K NIR MCD spectrum which exhibited two transitions, indicative of a tetrahedral high spin Fe(II) which is assigned to the isolated FeBrMes(SciOPP) complex. Addition of a second equivalent of MesMgBr resulted in a significant change in the 5 K NIR MCD spectrum, where three new transitions were observed. This spectrum was assigned to the isolated square planar Fe(II) S=1 $FeMes_2$(SciOPP) complex. When excess Grignard reagent was added to $FeCl_2$(SciOPP) (20 or 100 equiv.) a new feature was observed by MCD. This spectrum exhibited two negative bands and was assigned to the $FeMes_3^-$ complex. With an understanding of the species formed under stoichiometric reactions, the authors set to identify the species present in situ under catalytically relevant conditions. MCD spectra of time points obtained throughout the duration of the catalytic reaction show the initial formation of $FeMes_2$(SciOPP) which is then consumed over the course of 15 minutes resulting in just the FeIMes(SciOPP), as shown in Fig. 3. This led to a catalytic proposal where if 2 equivalents of MesMgBr were added to $FeCl_2$(SciOPP), the formation of $FeMes_2$(SciOPP) occurs. This complex is the active species of this reaction, reacting with the primary alkyl halide to form the C-C product and FeIMes(SciOPP). The mono-mesitylated species could then react with another equivalent of MesMgBr to reform the active bis-mesitylated species and continue the catalytic cycle.

In 2015, Neidig and co-workers used a similar approach to study iron–SciOPP catalysed Suzuki–Miyaura and Kumada cross-couplings of phenyl nucleophiles and secondary alkyl halides.[21] In this study,

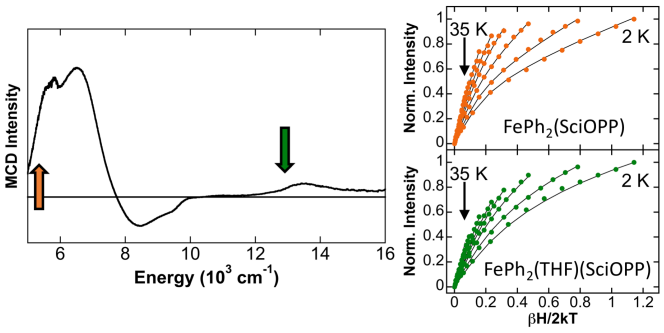

Fig 4. Left: The 5 K, 7 T, NIR MCD spectrum of the reaction of $FeCl_2$(SciOPP) with 2 equivalents of PhMgBr in 1:1 THF/2Me-THF. **Right**: Saturation magnetization data (dots) and fits (lines) collected at 5260 cm^{-1} (orange) and 13333 cm^{-1} in 1:1 THF/2Me-THF, used to assign the four and five coordinate complexes, respectively. Adapted with permission from *J. Am. Chem. Soc.*, 2015, **137**, 11432-11444 (https://pubs.acs.org/doi/abs/10.1021/jacs.5606648). Copyright 2015 American Chemical Society. Further permissions related to the material excerpted should be directed to the ACS.

similar iron species were observed in the 5 K NIR MCD spectra, namely FeIPh(SciOPP) and $FePh_2$(SciOPP) complexes. While the mono-phenylated species could be isolated and unambiguously characterized, this was not the case for the $FePh_2$(SciOPP) species. Instead, VTVH MCD was used to determine the coordination environment about the iron center when 2 equivalents of PhMgBr was added to $FeCl_2$(SciOPP)in situ. In THF, two species were observed by ^{57}Fe Mössbauer spectroscopy. However, when the reaction was performed in Et_2O, only one of the two species was observed suggesting the presence of a solvent adduct in THF. Using VTVH MCD, the four coordinate $FePh_2$(SciOPP) species was determined to be a high-spin distorted square pyramidal complex (Fig. 4). This is just one example which highlights the efficacy of VTVH MCD, as no other spectroscopic probe is available for determining the coordination number, oxidation state, and spin state of insitu generated paramagnetic organometallic species. Based on the reactivity and selectivity of the mono- and bis-phenylated iron species was investigated and it was determined that, while both complexes could form cross-coupled product, the selectivity towards C-C formation, as well as the low concentration of nucleophile in Suzuki–Miyaura and Kumada cross-coupling, suggests that the mono-phenylated FeIPh(SciOPP) complex is the dominant reactive species in these reactions, unlike the coupling of MesMgBr and primary alkyl halides.

Another example which highlights the unique ability of *C*-term MCD to allow for the characterization of unstable paramagnetic species which could not be isolated was the formation of three coordinate homoleptic iron alkyl complexes. These were found to be formed in the study of iron-catalysed cross-coupling reactions using simple iron salts and alkyl Grignard reagents.[22, 23] It had previously been reported by Neidig and co-workers that the reaction of $Fe(acac)_3$ with MeMgBr resulted in the formation of $FeMe_3^-$.[22] This species was isolated and characterized by single crystal X-ray crystallography as well as Mössbauer and MCD spectroscopy. The NIR MCD spectrum of $FeMe_3^-$ exhibited a unique double negative transition between 9000 and 10000 cm^{-1}. Additionally, the VTVH MCD of the isolated $FeMe_3^-$ complex fit to a S = 2 postive zero-field split non-Kramers doublet with ground-state Hamiltonion parameters of D = 13 ± 3 cm^{-1} and $|E/D|$ = 0.07 ± 0.03. Despite exhaustive efforts, the iron species formed upon reaction of $Fe(acac)_3$ with EtMgBr could not be isolated.[23] While the in situ Mössbauer parameters were similar for the in situ generated species formed with EtMgBr and the $FeMe_3^-$ complex, this was not enough evidence to assume the species formed was the analgous $FeEt_3^-$ species. To resolve this, Neidig and co-workers utilized *C*-term MCD spectroscopy of the in situ reaction of $Fe(acac)_3$ and EtMgBr. The authors found that this spectrum had the same double negative feature as was observed for the isolated $FeMe_3^-$ complex. When the VTVH data for the in situ reaction of $Fe(acac)_3$ and EtMgBr were analyzed, the data fit to similar parameters as the $FeMe_3^-$ complex. The fits were consistent with a S = 2 positive zero-field split non-Kramers doublet with ground-state Hamiltonion parameters of D = 13.2 ± 3 cm^{-1} and $|E/D|$ = 0.04 ± 0.03. From this data, the authors were able to determine that, much like in the reaction with MeMgBr, a homoleptic three coordinate iron species, $FeEt_3^-$ was formed in the reaction of $Fe(acac)_3$ with EtMgBr.

Subsequent studies extended the use of *C*-term MCD spectroscopy to study iron-catalysed cross-coupling reactions with NHC ligands. For example, in 2018 Neidig and co-workers reported the use of *C*-term MCD spectroscopy to investigate the differential reactivity observed across a series of *N*-heterocyclic carbene (NHC) ligands in iron catalysed alkyl-alkyl cross-coupling reactions.[24] The precatalyst of the reaction, using both IMes and SIMes NHCs, was a high spin iron(II) species which had additional iron-oxygen interactions from the acetal on the alkyl group of the Grignard reagent, resulting in divergent MCD features. It was later determined that, while the catalysis was quite selective using the mesityl NHC both saturated (SIMes) and unsaturated (IMes), if the isopropylphenyl NHCs (IPr or SIPr) were used, different selectivity was observed. When using the IPr NHC, similar yields and selectivity for C-C product was observed as those for the mesityl NHC reactions. When the SIPr NHC was used, the selectivity for the C-C product decreased drastically from that of the IPr, IMes, and SIMes reactions. These observations prompted further study of the electronic structure and bonding of the precatalyst using each of these four NHC ligands to try to explain this divergent reactivity (Fig.5).

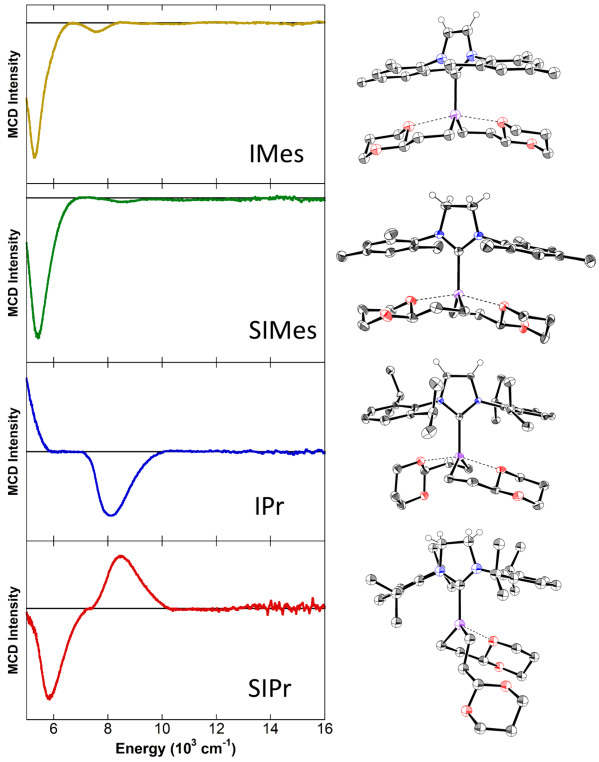

Fig 5. The 5 K, 7 T, NIR MCD spectra (left) and structures (right) of the high spin iron(II) NHC complexes. Adapted with permission from *Organometallics.*, 2018, **37**, 3093-3101. Copyright 2018 American Chemical Society.

Electronic Structure and Bonding in Paramagnetic Transition Metal Organometallics

While recent studies have utilized *C*-term MCD to provide a better understanding of the reactivity and underlying mechanism of catalysis with paramagnetic organometallics, this experiment has traditionally been utilized to provide fundamental electronic structure insight in isolated paramagnetic organometallic complexes. Most notably, this technique has provided detailed insight into the effect of ligand perturbation and ligand type in several iron and cobalt paramagnetic complexes highlighted herein. It has also been utilized for understanding the electronic structure and bonding interactions of redox flexible ligands, where the metal-ligand bonding is often difficult to spectroscopically characterize. While the examples herein focus on the low energy NIR region of the MCD spectra, where the d-d transitions are observed, it is also important

to note that this technique is equally as insightful in the UV-vis region. In this high energy region, *C*-term MCD provides high resolution spectra of the MLCT and LMCT transitions which allows for a more detailed understanding of metal-ligand interactions in paramagnetic organometallic species.

As previously mentioned, the divergent reactivity in iron catalysed C-C cross-coupling when using the SIPr ligand when compared to the IPr, IMes, and SIMes analogues prompted a more in-depth study of these iron NHC complexes. Isolation of the precatalyst for the SIPr reaction showed that the additional steric requirement of the saturated NHC backbone only allowed for one of the iron-oxygen interactions which seemingly results in poor selectivity for the C-C bond formation. With this in mind, this series of iron-NHC complexes allowed for investigation of the fundamental understanding of electronic structure and bonding across these NHC ligands using *C*-term MCD spectroscopy combined with DFT and ^{57}Fe Mössbauer spectroscopy.[25] When comparing the *C*-term MCD of the IPr and SIPr complexes it was determined that the IPr complexes displayed two temperature dependent *C*-term MCD signals while the SIPr complex displayed *C*-terms of opposite intensity, resulting in a pseudo *A*-term. This is consistent with the change in ligand field from the pseudo 5-coordinate complex to the pseudo 4-coordinate complex. The average ligand field energy in the SIPr complex was also larger, which is consistent with the SIPr complex having a more covalent ligand environment. This was further supported by the shortened Fe-C bonds observed crystallographically for the SIPr complex when compared to the IPr analogue. The conclusion based on the information obtained from the combination of these experiments was that altering the NHC electronics has little effect on the electronic structure of these iron complexes. Instead, the steric demand required by the saturated backbone of SIPr in combination with the bulky isopropylphenyl ligands altered the chelation of the alkyl substrate. This inhibition of the chelation of both of the alkyl ligands prevented the formation of the key precatalyst and therefore would not allow for formation of cross-coupled product.

Several other iron catalysed cross-coupling reactions utilize the NHC ligand scaffold, with examples ranging from aryl-aryl, alkyl-aryl, and alkyl-alkyl couplings. In many of these systems, it is observed that the saturation of the backbone of the NHC can have quite an effect on the resulting product yields. For example, Nakamura and co-workers reported a decrease of nearly 30% yield when using SIPr instead of IPr in their 2012 report of iron catalysed alkyl-aryl cross coupling.[26] Understanding the electronic structure of the active species, and if the effect observed is due to electronic or steric effects, can help guide future methodology. An example of this was published in 2015 by Neidig and co-workers studied the effect of backbone electronics across a series of three coordinate high spin iron NHC alkyl complexes of the type (NHC)Fe(CH_2TMS)$_2$.[27] Here, the NHC backbone was varied, using the saturated SIPr, the unsaturated IPr, and the chlorinated ^{Cl}IPr ligands. The NIR *C*-term MCD spectra of these complexes were all very similar, displaying two negative bands with small shifts in energy across the series (Fig. 6). The UV-vis MCD region also showed little changed in the charge transfer transitions across this series. These results in combination with VTVH MCD, ^{57}Fe Mössbauer spectroscopy and DFT, determined that the change in backbone electronics had little effect on the electronic structure of the iron(II) center.

In addition to providing insight into three coordinate iron NHC complexes, this study also investigated four coordinate iron NHC complexes. It had previously been suggested that NHCs may be stronger field ligands than phosphine ligands and therefore may be alternatives in the development of iron-based catalysts. This study allowed for the direct comparison of a series of tetrahedral iron dichloride complexes with varying supporting ligands including two phosphine, two diamine, and two NHC complexes.[27] The combined MCD and DFT techniques allowed for the first direct elucidation of the value of 10Dq for these types of complexes, providing direct insight into the ligand field strength of the NHC when compared to phosphine and diamine ligands. It was found that the iron NHC complexes had a strong trans effect, which had been previously proposed but not experimentally determined. With this, the NHC ligand resulted in a weakening of the Fe-Cl bond and an overall decrease the value of the 10Dq. Overall, with the use of MCD spectroscopy and DFT, it was determined that the NHC is not a simple analogue of the phosphine ligand for iron as it was once thought to be. The direct evidence of the trans effect of the NHC also suggests that, when using the NHC ligand, the rate of transmetallation would be faster than that of the phosphine or diamine ligands due to the weakening of the Fe-X bond which may allow for unique reactivity in iron cross-coupling reactions.

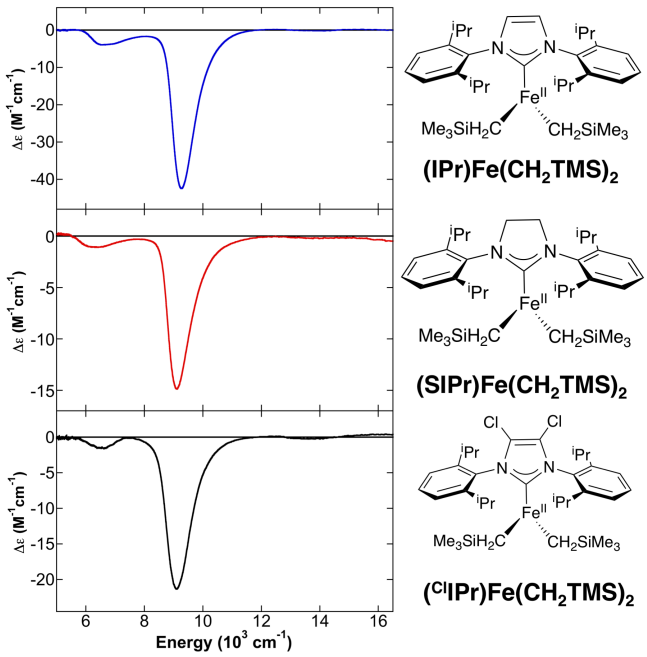

Fig 6. The 5 K, 7 T, NIR MCD spectra and structures of the three-coordinate iron NHC complexes. *Chem. Sci.*, 2015, **6**, 1178-1188. Published by the Royal Society of Chemistry.

In addition to the well-known isopropylphenyl and mesityl NHC ligands, NHC-pincer type ligands have also been investigated using *C*-term MCD spectroscopy in combination with DFT and ^{57}Fe Mössbauer spectroscopy. These NHC-containing pincer ligands were designed in an attempt to generate a more oxidatively robust pincer scaffold which should in turn result in new catalytic reactivity. In order to understand this reactivity, understanding the electronic structure and bonding of the ligands with the iron is essential. The influence of NHC moieties in the tridentate pincer ligand on electronic structure and bonding in (pincer)$FeBr_2$ complexes were investigated (pincer = bis(imino)pyridine (PDI), bis(amidinato)-N-heterocyclic carbene (CDA), or bis(N-heterocyclic carbene)pyridine (CNC)). These complexes provided one example with no NHC ligands, one example with one NHC ligand, and one example with two NHC ligands for a comparison of the effect of the NHC ligand on the pincer

moiety. The combined use of *C*-term NIR and VTVH MCD allowed for the determination of the spin state, ligand field strengths and ZFS parameters of these three iron complexes (Fig. 7).[28] The (^{iPr}PDI)FeBr$_2$ and (^{iPr}CNC)FeBr$_2$ complexes displayed two transitions in the NIR MCD spectra, consistent with high spin (S = 2) Fe(II) complexes. This spin state assignment was confirmed using VTVH MCD.

The NIR MCD spectrum of (^{iPr}CDA)FeBr$_2$ contains five transitions

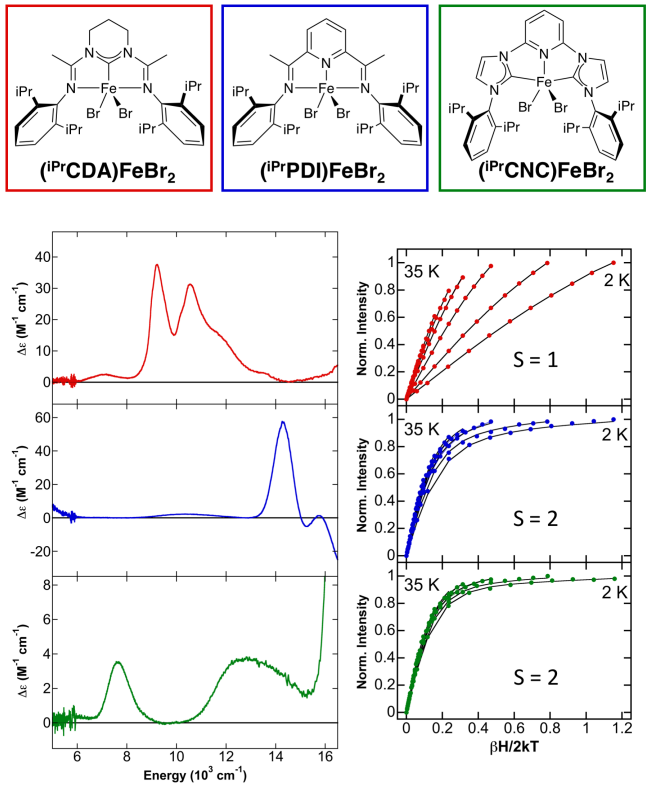

Fig 7. Top: Structures of the iron NHC pincer complexes; **Left:** The 5 K, 7 T, NIR MCD spectra; **Right:** Saturation magnetization data collected at 9217 cm^{-1}, 13889 cm^{-1}, and 7634 cm^{-1}, respectively. Adapted with permission from *Organometallics*, 2016, **35**, 3692-3700. Copyright 2016 American Chemical Society.

more than would be expected for a high spin Fe(II) complex, but is consistent with an intermediate spin (S = 1) Fe(II) complex. Like the (^{iPr}PDI)FeBr$_2$ and (^{iPr}CNC)FeBr$_2$ complexes, the S = 1 spin state of (^{iPr}CDA)FeBr$_2$ was confirmed with VTVH MCD. When comparing the two S = 2 systems, an increased ligand field strength, and therefore ligand field splitting, is observed when comparing of (^{iPr}PDI)FeBr$_2$ and (^{iPr}CNC)FeBr$_2$. When the complex contains the ^{iPr}CNC ligand, the ligand field splitting ($10Dq \approx 10\,555$ cm^{-1}) was observed to be much larger than with the ^{iPr}PDI ligand ($10Dq \leq 7700$ cm^{-1}), indicating that the ^{iPr}CNC ligand has a larger ligand field than the ^{iPr}PDI ligand in this series. This increase was attributed to the increasing σ donation of the NHC ligands than that of the pyridine in (^{iPr}PDI)FeBr$_2$ but was not large enough to result in a change in the spin state as observed in the ^{iPr}CDA complex. This suggested that the net donor ability of the pincer ligand is not directly correlated to the number of NHC ligands and instead is more dependent on the orientation of the NHC in the pincer structure which maximizes the metal-ligand interactions in the ^{iPr}CDA complex. This understanding that the orientation of the NHC ligand in the pincer ligand scaffold changes the donor ability of the ligand provided important insight for the future of ligand design in organometallic catalysis.

The use of *C*-term MCD spectroscopy for understanding electronic structure and bonding in organometallic chemistry has also been extended to other transitions metals. Similar to the iron NHC complexes, cobalt NHC complexes have shown promising catalytic activity in areas such as C-H functionalization as well as cross-coupling but have been lesser studied than their phosphine analogues. As previously shown for iron, a fundamental understanding of the electronic structure and bonding of organometallic complexes allows for educated and improved ligand design. In 2017, Neidig and co-workers utilized *C*-term MCD in combination with DFT calculations to gain insight into the electronic structure and bonding of a series of cobalt NHC complexes.[29] The MCD spectrum of the (IMes)$_2$CoCl$_2$ features six transitions, three low-energy and three high-energy transitions (Fig. 8, top). This is consistent with the distorted tetrahedral high spin Co(II) (S = 3/2), which has a characteristic spectrum with strong negative signal and series of positive signals at higher energies.[30] The *C*-term MCD experiment was also used to determine the ligand field strength in (ICy)$_2$CoCl$_2$ (ICy = 1,3-dicyclohexylimidazol-2-ylidene) to determine the effect of N-substituent on NHC complexes and (dppp)CoCl$_2$ (dppp = 1,3-bis(diphenylphosphino)propane) to compare ligand field strength of the NHC ligands with a bisphosphine ligand. The MCD spectra of all complexes display the same general features, suggesting that all are distorted tetrahedral high spin Co(II) complexes. In a comparison of the NIR MCD spectra of (ICy)$_2$CoCl$_2$ and (IMes)$_2$CoCl$_2$, the low energy transitions are shifted towards

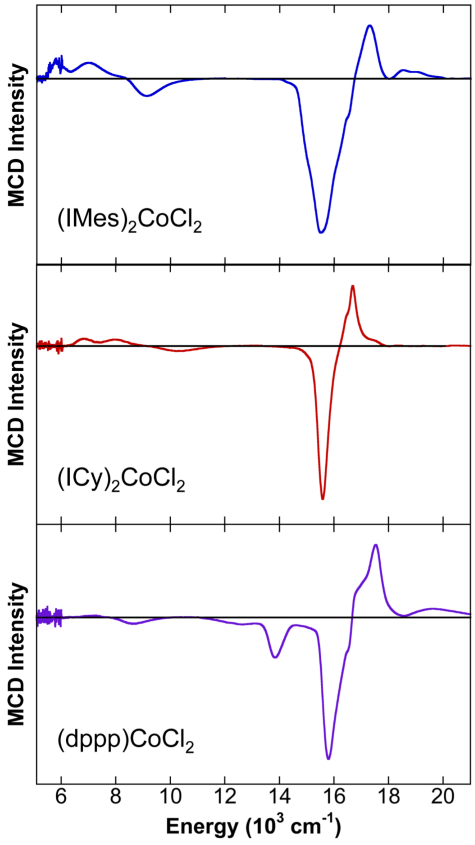

Fig 8. The 5 K, 7 T, NIR MCD spectra of the cobalt NHC complexes. Reproduced from Ref. 26 with permission from The Royal Society of Chemistry.

higher energies ~1000 cm^{-1}, while the higher energy transitions are slightly shifted towards lower energies (Fig 8, middle and bottom). This suggests that the N-substituent has a significant effect on the NHC bonding, likely due to the steric effects of the substituent. In the spectrum of (dppp)$CoCl_2$ all transitions are shifted towards higher energies, which suggests the bisphosphine ligand can provide a stronger ligand field to cobalt than the NHC ligands.

In addition to the study of organometallic cobalt complexes, *C*-term MCD has been used to provide more detailed insight into the absorption features of vanadocene.[31] In 2012, Jackson, Telser and co-workers sought to further elucidate the electronic structure of vanadocene, or bis(η^5-cyclopentadienyl)vanadium(II). This complex had been previously investigated in the late 1960s and the advances in both spectroscopic and computational technologies utilized in 2012 allowed for the definitive description of the electronic structure of this important organometallic complex. While several spectroscopic probes were utilized in this study, along with computational insight, the *C*-term MCD spectrum was specifically used to confirm the assignments which were previously made of the absorption spectrum. The MCD spectrum, in combination with multireference *ab initio* methods verified that the assignments reported in the 1960s were correct. The insight provided also confirmed the original proposal that the e_{2g} molecular orbitals are lower in energy than the a_{1g} molecular orbitals. This had been in question due to DFT calculations which had been reported between the original 1960s study and this 2012 study, outlining the importance of combining DFT calculations with experimental data.

Paramagnetic f-element Organometallics

Despite the significant advancements in the synthesis of organometallic complexes featuring f-block elements, and their unique reactivity and prevalence in nuclear fuel waste, analysis of their electronic structure and bonding remains underdeveloped in comparison to their d-block analogues. The information obtained from thorough investigations of the electronic structure and bonding in f-element organometallics is central to understanding the experimentally observed reactivity as well as for guiding ligand design for separations chemistry. Of primary interest in this area is a fundamental understanding of the f-orbital participation in bonding, an area which requires a large variety of complexes with unique ligands sets, as well as those with the same ligand set and various f-elements, to directly compare the metal ligand interactions across a series of molecules. This variety of systematically unique complexes can be achieved in organometallic chemistry, where control of the coordination environment can be maintained while a broad range of ligands are introduced.

While there are these series available, the ability to directly probe the f-orbital participation is difficult. The highly paramagnetic nature of many of the f-block oxidation states makes traditional spectroscopic probes, such as NMR, difficult to interpret. The f-f transitions are Laporte forbidden and therefore are often very low in intensity, if they can be observed at all in traditional absorption spectroscopy. In contrast, NIR *C*-term MCD allows for the direct observation of the f-f transitions in paramagnetic organometallic f-block complexes and, when combined with theoretical calculations, these transitions have been successfully assigned. The UV-vis *C*-term MCD allows for observation of f-d and LMCT and MLCT bands in complexes which the absorption spectra are overwhelmed by the ligand-based transitions. This experiment was first utilized by Denning and co-workers in the study of $NpO_2Cl_2^-$ and $NpO_2(NO_3)_3^-$.[32, 33] While not an organometallic complex, the MCD experiment has recently been utilized by Slageren, Pereira and co-workers to provide electronic structure insight in the uranium (III) single-ion magnet. In this study, when combining MCD with ab initio insight, the authors determined that this complex contains a mixed ground state configuration where the ±7/2 and ±5/2 states dominate with a small contribution from the ±1/2.[34] Recent examples of the utility of *C*-term MCD in studying the electronic structure and bonding in f-element organometallics are outlined below.

Electronic Structure and Bonding in paramagnetic f-element Organometallic Complexes

It has recently been discovered that the chemical reduction of a series of Ln(III) tris(silylcyclopentadienyl) complexes using potassium graphite in the presence of a cation complexant results in the formation of the formal +2 oxidation state for all the traditional lanthanide ions**,** with the exception of radioactive Pm. The successful reduction of these complexes was unexpected, as the predicted reduction potentials of the Ln(III)/Ln(II) redox pair were greater than the -2.9 V vs SHE of potassium. However, these values were calculated using the $4f^n \rightarrow 4f^{n+1}$ reduction, whereas structural, spectroscopic, and magnetic data, as well as DFT analysis, suggest the reduction involves the addition of an electron to a 5d orbital, $4f^n \rightarrow 4f^n5d^1$.

The electronic structure of these Ln(II) complexes were

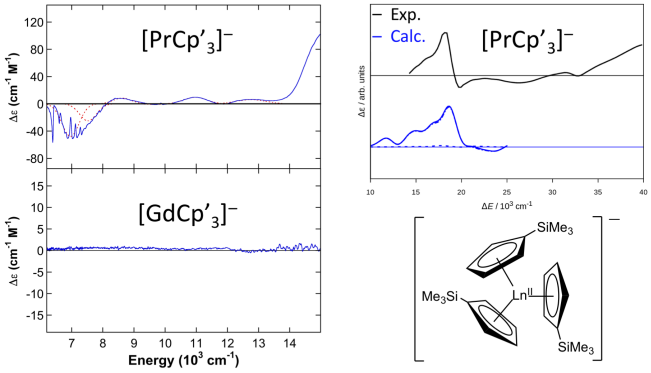

Fig 9. The 5 K, 7 T, NIR MCD of the Pr and Gd Cp' complexes (left). The experimental (black) and calculated (blue) UV-vis MCD spectrum of $[PrCp'_3]^-$ (top right) and general structure of the complexes (bottom right). Adapted with permission from *Organometallics*, 2019, **38**, 3124-3131. Copyright 2019 American Chemical Society.

investigated using a combined experimental and computational approach, combining experimental MCD spectroscopy with restricted active-space (RAS) calculations to gain further insight into the electronic structure and ground state of the Y(II), La(II), Pr(II), Eu(II), and Gd(II) complexes (Fig. 9, bottom right).[35] The Pr complex exhibited at least five transitions in the NIR MCD spectrum (Fig. 9, top left). These transitions are consistent with the low-energy Laporte-forbidden f-f transitions. The appearance of these transitions is consistent with the presence of unpaired f-electrons in the ground state of the Pr(II) complex, consistent with the previously reported $4f^25d^1$ ground state. The Y, La, Eu, and Gd complexes exhibited no signal in the 5 K NIR MCD spectra (Fig 9, bottom left).

This is consistent with the $4f^n5d^1$ which had been previously assigned. Here, the ground state of the Y and La complexes would be $4d^1$ and $5d^1$, respectively, and the ground state of the Eu and Gd complexes are $4f^7$ and $4f^75d^1$, respectively. If the ground states of these complexes followed the traditional $4f^{n+1}$ rule, the ground state of the Gd complex would instead be $4f^8$, resulting in 1 unpaired electron in the f-orbitals and observed f-f transitions in the NIR MCD. The lack of f-f transitions in the MCD supports the $4f^75d^1$ ground state, where all f-orbitals are half filled and therefore the f-f transitions are spin forbidden.

The higher energy UV-vis MCD spectra of the Y, Pr, and Gd complexes were probed using experimental MCD spectra and RAS calculations (Fig 9, top right). Previously reported electronic absorption spectra of these complexes were very broad, making assignment of the transitions in this region very difficult. The higher resolution MCD experiment allowed for the separation of peaks which had been previously assigned as d-d and d-π* transitions. To support these assignments, RAS calculations were performed to predict the UV-vis MCD spectra that were in good agreement with the experimentally observed data. From these calculations, the observed transitions for all three complexes were able to be assigned and previously reported assignments confirmed. This study allowed for confirmation of previously reported ground state insight into the unique Ln(II) ground state and showed the power of MCD spectroscopy, when combined with theoretical calculations, in collecting high resolution absorption data and assigning the transitions observed experimentally.

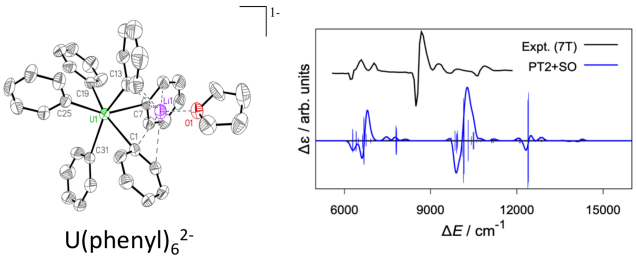

Fig 10. The structure (left) and the experimental (black) and calculated (blue) NIR MCD spectrum of UPh_6^{2-}. Adapted with permission from Ref. 33. Copyright 2019 Wiley-VCH Verlag GmbH & Co. KGaA.

The combined experimental and computational MCD approach has also been applied in organometallic uranium complexes. In 2019, Neidig, Autschbach and co-workers reported the synthesis and characterization of a series of homoleptic uranium (IV) aryl complexes of the form $U(Ar)_6^{2-}$ (Ar = phenyl, *p*-tolyl, *p*-Cl-phenyl).[36] These complexes marked the first structurally characterized, sterically unencumbered homoleptic uranium (IV) aryl-ate complexes. This study focused on the NIR region of the MCD, where the f → f transitions were observed, and benchmarked the first report of both experimental and theoretical uranium (IV) *C*-term MCD spectra. The experimental NIR MCD of the three uranium(IV) aryl complexes displayed very similar features. Due to an inner-sphere lithium cation interaction, the phenyl and *p*-tolyl complexes underwent very similar structural distortions. These two complexes exhibited identical NIR MCD spectra, suggesting that the more electron donating *p*-tolyl ligand had little effect with respect to the phenyl complex on the metal interactions between the uranium center and the aryl ligands.

The *p*-Cl-phenyl complex did not undergo the same structural distortion as it did not have the inner-sphere lithium cation. A comparison of the *p*-Cl-phenyl NIR MCD spectrum to that of the phenyl complex showed that the *p*-Cl-phenyl had very similar metal-ligand interactions to the phenyl complex, but with broader signals. This is likely to be due to the assent in symmetry due to the lack of the inner-sphere lithium distortion in the *p*-Cl-phenyl complex. Like the *p*-tolyl complex, this result suggested that the more electron withdrawing *p*-Cl-phenyl ligand had very little effect on the metal-ligand interactions when compared to the phenyl complex. In addition to the experimental NIR MCD spectra, calculated NIR MCD spectra of all three complexes supported the similarities observed experimentally (Fig. 10). It was determined that all three complexes have the same ^3H free-ion ground state term and that the transitions observed in all three complexes were indeed f-f transitions and were of the same parentage across the series. Overall this study suggested that the NIR MCD spectra was much more dependent geometry and oxidation state and remained unperturbed by the changes in the ligand environments.

Extending this type of combined approach to other oxidation states and ligand environments in uranium chemistry is important, as each oxidation state has unique reactivity and bonding interactions important for both reactivity and ligand design for isotope separation. Recently, the combination of MCD, EPR, and computational insight, was utilized to study the electronic structure of a series of U(III) tris(3,5-dimethyl-1-pyrazolyl)borate (Tp*) complexes.[37] Much like the U(IV) aryl complexes, it was found that the perturbation of the ligand environment, for example when exchanging the iodine in Tp^*_2UI with a benzyl (Bn) group to make Tp^*_2UBn, has little effect on the overall electronic structure. The three U(III) complexes, Tp^*UI_2, Tp^*_2UI, and Tp^*_2UBn displayed similar *C*-term features in the NIR region of the MCD. In the UV-vis region, TD-DFT calculations allowed for assignment of the absorption bands, which were similar across the series as well. In addition, this combined approach was utilized to redefine the ground state of a U(III) complex with a redox non-innocent bipyridine ($Bipy^-$) ligand, Tp^*_2UBipy. By combining EPR and MCD studies with DFT calculations, it was determined that there was antiferromagnetic coupling of the ligand radical of the $Bipy^-$ ligand with the unpaired electron of the U(III) center.

The combination of *C*-term MCD with other spectroscopic techniques, as well as computational insight, has proven powerful in understanding the metal ligand interactions in uranium complexes of varying oxidation states and ligand environments. The information gained from these studies is important for understanding the reactivity observed for uranium in its various oxidation states as well as for designing ligands for isotope separations in nuclear fuel waste. Further expansion of this approach across a variety of oxidation states, ligand environments, and geometries across the lanthanide and actinide series in the future will allow for further fundamental insight into the effect, or lack thereof, of the ligand environment in organometallic f-element chemistry.

Conclusions

The use of *C*-term MCD has shown great success in studying the electronic structure and bonding both of isolated complexes as well as of in situ generated species in paramagnetic organometallic chemistry. While there are several examples that show the efficacy of this technique, its utilization is still in its infancy. In transition metal chemistry, the use of *C*-term MCD spectroscopy for elucidating electronic structure of in situ generated intermediates has remained limited to a few examples with iron and just one example with nickel. Extending the use of *C*-term MCD to include catalytic systems of

other transition metals is of particular interest. Nickel has recently been highlighted for its use as a catalyst in both traditional cross-coupling as well as cross-electrophile coupling, where paramagnetic Ni(I)/Ni(III) intermediates are proposed.[38] In these systems, the use of MCD would allow for the determination of the coordination number and geometry of the active species in these systems. Additionally, cobalt has been shown to effectively catalyse both cross-coupling transformations, as well as C-H activation reactions.[39, 40] Much like in the nickel case, utilizing *C*-term MCD for the study of insitu speciation in the cobalt systems could provide invaluable insight into the active species in these transformations. In addition, the combination of stopped-flow rapid freeze-quench with *C*-term MCD, a combination often utilized in bioinorganic chemistry, would allow for determination of very short lived intermediates in metal catalysed transformations. The use of *C*-term MCD could provide valuable insight into the electronic structure and bonding of the reactive intermediates, allowing for more rational design of ligands for catalysis.

This technique has also been shown to be effective for studying the electronic structure and bonding in f-element complexes, specifically in lanthanides as well as uranium complexes. In these areas, extension of this technique to f-element organometallics with a wider variety of ligands across multiple oxidation states would be of interest to systematically determine the effects of both ligand and oxidation state on the electronic structure. Additionally, utilizing *C*-term MCD to obtain information about the in situ speciation of uranium complexes in uranium-mediated transformations, as well as in small molecule activation, is of great interest and ongoing. As shown by Denning and co-workers with neptunium, *C*-term MCD can also be utilized to provide electronic structure and bonding information in transuranic species. This area has not yet been widely explored but could be of great interest to the actinide community to better understand covalency and bonding in transuranic organometallic species.

A fundamental understanding of the electronic structure and bonding in d- and f-block organometallic complexes is critical for the rational development of new ligands and complexes for applications ranging from small molecule reactivity and catalysis to nuclear waste separations. Towards this goal, *C*-term MCD spectroscopy has emerged as a powerful method to elucidate electronic structure in paramagnetic d- and f-block organometallics. This perspective has highlighted several recent applications in this field, including the utility of this method in studies of transient and reactive species. Expanding the use of *C*-term MCD across both the d- and f-block will assuredly provide important insight into the structure-function relationships, guiding both reactivity as well as ligand design for future methodology design and separations chemistry.

Conflicts of interest

The authors declare no conflicts of interest.

Acknowledgements

M.L.N. acknowledges support for this work from the U.S. Department of Energy, Office of Science, Early Career Research Program under Award DE-SC0016002, the National Institutes of Health (R01GM111480), and the National Science Foundation (CHE-1954480).

Notes and references

1. J. G. Dawber, *Analyst*, 1964, **89**, 755-762.
2. N. Kobayashi and K. Nakai, *Chem. Commun.*, 2007, DOI: 10.1039/B704991A, 4077-4092.
3. J. a. S. Mack, M.J., in *Encyclopedia of Inorganic and Bioinorganic Chemistry*, ed. R. A. Scott, DOI: 10.1002/9781119951438.eibc0289.
4. E. G. Pavel and E. I. Solomon, in *Spectroscopic Methods in Bioinorganic Chemistry*, American Chemical Society, 1998, vol. 692, ch. 6, pp. 119-135.
5. E. Solomon, M. Neidig and G. Schenk, *Compr. Coord. Chem. II*, 2004, **2**.
6. E. I. Solomon, T. C. Brunold, M. I. Davis, J. N. Kemsley, S.-K. Lee, N. Lehnert, F. Neese, A. J. Skulan, Y.-S. Yang and J. Zhou, *Chem. Rev.*, 2000, **100**, 235-350.
7. E. I. Solomon, E. G. Pavel, K. E. Loeb and C. Campochiaro, *Coord. Chem. Rev.*, 1995, **144**, 369-460.
8. L. B. LaCroix, S. E. Shadle, Y. Wang, B. A. Averill, B. Hedman, K. O. Hodgson and E. I. Solomon, *J. Am. Chem. Soc.*, 1996, **118**, 7755-7768.
9. J. McMaster, M. D. Carducci, Y.-S. Yang, E. I. Solomon and J. H. Enemark, *Inorg. Chem.*, 2001, **40**, 687-702.
10. M. L. Neidig, M. Kavana, G. R. Moran and E. I. Solomon, *J. Am. Chem. Soc.*, 2004, **126**, 4486-4487.
11. E. I. Solomon, *Inorg. Chem.*, 2001, **40**, 3656-3669.
12. M. G. I. Galinato, E. P. Brocious, F. Paulat, S. Martin, J. Skodack, J. B. Harland and N. Lehnert, *Inorg. Chem.*, 2020, **59**, 2144-2162.
13. M. W. Wolf, K. Rizzolo, S. J. Elliott and N. Lehnert, *Biochemistry*, 2018, **57**, 6416-6433.
14. J. Yang, R. Rothery, J. Sempombe, J. H. Weiner and M. L. Kirk, *J. Am. Chem. Soc.*, 2009, **131**, 15612-15614.
15. C. J. Barrows, V. A. Vlaskin and D. R. Gamelin, *J. Phys. Chem. Lett.*, 2015, **6**, 3076-3081.
16. K. H. Hartstein, A. M. Schimpf, M. Salvador and D. R. Gamelin, *The J. Phys. Chem. Lett.*, 2017, **8**, 1831-1836.
17. T. A. Jackson, E. Yikilmaz, A.-F. Miller and T. C. Brunold, *J. Am. Chem. Soc.*, 2003, **125**, 8348-8363.
18. T. A. Stich, N. R. Buan and T. C. Brunold, *J. Am. Chem. Soc.*, 2004, **126**, 9735-9749.
19. J. Shin, S. Gwon, S. Kim, J. Lee and K. Park, *J. Am. Chem. Soc.*, 2020, **142**, 4173-4183.
20. S. L. Daifuku, M. H. Al-Afyouni, B. E. R. Snyder, J. L. Kneebone and M. L. Neidig, *J. Am. Chem. Soc.*, 2014, **136**, 9132-9143.
21. S. L. Daifuku, J. L. Kneebone, B. E. R. Snyder and M. L. Neidig, *J. Am. Chem. Soc.*, 2015, **137**, 11432-11444.
22. S. B. Muñoz III, S. L. Daifuku, J. D. Sears, T. M. Baker, S. H. Carpenter, W. W. Brennessel and M. L. Neidig, *Angew. Chem. Int. Ed.*, 2018, **57**, 6496-6500.
23. J. D. Sears, S. B. Muñoz III, S. L. Daifuku, A. A. Shaps, S. H. Carpenter, W. W. Brennessel and M. L. Neidig, *Angew. Chem. Int. Ed.*, 2019, **58**, 2769-2773.
24. V. E. Fleischauer, S. B. Muñoz Iii, P. G. N. Neate, W. W. Brennessel and M. L. Neidig, *Chem. Sci.*, 2018, **9**, 1878-1891.
25. S. B. Muñoz, V. E. Fleischauer, W. W. Brennessel and M. L. Neidig, *Organometallics*, 2018, **37**, 3093-3101.
26. S. K. Ghorai, M. Jin, T. Hatakeyama and M. Nakamura, *Org. Lett.*, 2012, **14**, 1066-1069.
27. K. L. Fillman, J. A. Przyojski, M. H. Al-Afyouni, Z. J. Tonzetich and M. L. Neidig, *Chem. Sci.*, 2015, **6**, 1178-1188.
28. T. M. Baker, T. L. Mako, A. Vasilopoulos, B. Li, J. A. Byers and M. L. Neidig, *Organometallics*, 2016, **35**, 3692-3700.
29. T. E. Iannuzzi, Y. Gao, T. M. Baker, L. Deng and M. L. Neidig, *Dalton Trans.* 2017, **46**, 13290-13299.

30. H. Kato and K. Akimoto, *J. Am. Chem. Soc.*, 1974, **96**, 1351-1357.
31. T. A. Jackson, J. Krzystek, A. Ozarowski, G. B. Wijeratne, B. F. Wicker, D. J. Mindiola and J. Telser, *Organometallics*, 2012, **31**, 8265-8274.
32. R. G. Denning, J. O. W. Norris and D. Brown, *Mol. Phys.*, 1982, **46**, 287-323.
33. R. G. Denning, J. O. W. Norris and D. Brown, *Mol. Phys.*, 1982, **46**, 325-364.
34. J. T. Coutinho, M. Perfetti, J. J. Baldoví, M. A. Antunes, P. P. Hallmen, H. Bamberger, I. Crassee, M. Orlita, M. Almeida, J. van Slageren and L. C. J. Pereira, *Chem. Eur. J.*, 2019, **25**, 1758-1766.
35. V. E. Fleischauer, G. Ganguly, D. H. Woen, N. J. Wolford, W. J. Evans, J. Autschbach and M. L. Neidig, *Organometallics*, 2019, **38**, 3124-3131.
36. N. J. Wolford, D.-C. Sergentu, W. W. Brennessel, J. Autschbach and M. L. Neidig, *Angew. Chem. Int. Ed*, 2019, **58**, 10266-10270.
37. N. J. Wolford, X. Yu, S. C. Bart, J. Autschbach and M. L. Neidig, *Dalton Trans*, 2020, **49**, 14401-14410.
38. J. B. Diccianni and T. Diao, *Trends Chem.*, 2019, **1**, 830-844.
39. G. Cahiez and A. Moyeux, *Chem. Rev.*, 2010, **110**, 1435-1462.
40. M. Moselage, J. Li and L. Ackermann, *ACS Catal.*, 2016, **6**, 498-525.